ELSEVIER

Biochimica et Biophysica Acta 1190 (1994) 99–107

BBA Biochimica et Biophysica Acta

Effect of liposome size on the circulation time and intraorgan distribution of amphipathic poly(ethylene glycol)-containing liposomes

David C. Litzinger [a,1], Antoinette M.J. Buiting [b], Nico van Rooijen [b], Leaf Huang [a,*]

[a] *Department of Pharmacology, University of Pittsburgh School of Medicine, Pittsburgh, PA 15261, USA*
[b] *Department of Cell Biology and Immunology, Medical Faculty, Vrije Universiteit, Amsterdam, The Netherlands*

(Received 24 June 1993)
(Revised manuscript received 4 October 1993)

Abstract

Liposomes containing dioleoyl-*N*-(monomethoxypoly(ethylene glycol)succinyl)-phosphatidylethanolamine (PEG-PE), and of three characteristic sizes ($d > 300$ nm, $d \sim 150$–200 nm, and $d < 70$ nm), were prepared, injected into mice, and their biodistributions examined following a radioactive lipid phase marker. The large and small liposomes accumulated to elevated levels in spleen and liver, respectively. The intermediate sized liposomes were found to be the longest circulating. Furthermore, when injected into mice bearing murine MC-38 colon carcinoma tumor, an approximate 2-fold increase in the % injected dose per g tumor was observed for the long-circulating liposomes compared to liposomes without PEG-PE. The distribution of the injected liposomes within the tumor was examined by fluorescence microscopy, where the liposomes were labeled with 1,1′-dioctadecyl-3,3,3′,3′-tetramethylindocarbocyanine perchlorate (DiI). The liposomes were found surrounding blood vessels in the tumor, with some degree of extravasation into the tumor mass. A previous explanation for the reduced circulation time of small liposomes has been that they have an ability to pass through the fenestrated liver endothelium and thereby reach the parenchymal cells. DiI-labeled liposomes were therefore used to examine the intrahepatic distribution of the injected liposomes. Liposomes accumulated in liver were localized to Kupffer cells, regardless of liposome size. The small liposomes were not detectable in areas comprised of parenchymal cells when using this fluorescence technique. The reason for reduced long-circulating behavior for the small liposomes may be more directly related to the activity of PEG-PE. Therefore the steric barrier activity of the liposomes was examined by a serum protein binding assay and by streptavidin binding to biotinylated liposomes. The steric barrier was liposome size dependent, with the small liposomes revealing increased protein binding. This decreased steric barrier of the small liposomes may result in increased susceptibility to opsonization and thus explain their more rapid clearance from the circulation. The large liposomes accumulated in spleen were localized in the red pulp and marginal zone. Uptake of the large liposomes may occur by means of a filtration mechanism. These results establish the significance of liposome size in determining liposome circulation time and biodistribution, and are relevant for the optimal design of liposomes for drug delivery.

Key words: Poly(ethylene glycol); Liposome; Biodistribution; Drug delivery

* Corresponding author. Fax: + 1 (412) 6481945.
[1] Present address: Amgen, Inc., 1840 DeHavilland Dr., Thousand Oaks, CA 91320, USA.

Abbreviations: biotin-cap-PE, biotinamidocaproylphosphatidylethanolamine; CEA, carcinoembryonic antigen; Chol, cholesterol; DiI, 1,1′-dioctadecyl-3,3,3′,3′-tetramethylindocarbocyanine perchlorate; DOPE, dioleoylphosphatidylethanolamine; DSPE, distearoylphosphatidylethanolamine; DTPA-SA, diethylenetriaminepentaacetic acid stearylamide; EPC, egg phosphatidylcholine; FITC, fluorescein isothiocyanate; ^{3}H-CE, hexadecyl [^{3}H]cholestanyl ether; PBS, phosphate-buffered saline; PEG, poly(ethylene glycol); PEG-PE, dioleoyl-*N*-(monomethoxypoly(ethylene glycol)succinyl) phosphatidylethanolamine; RES, reticuloendothelial system.

SSDI 0005-2736(93)E0311-W

1. Introduction

Incorporation of amphipathic poly(ethylene glycol) (PEG) conjugates in liposome bilayers has been shown to prolong liposome circulation [1–3]. Such long-circulating liposomes are able to accumulate in solid tumor [4–6]. Furthermore, the therapeutic efficacy of antitumor drug encapsulated in these liposomes is significantly greater than either drug entrapped in con-

ventional liposomes or free drug in the treatment of mice bearing colon carcinoma [4,6]. It has been proposed that the amphipathic PEG may provide a steric barrier [7,8] as well as increase the hydrophilicity [1,3] of the liposome surface. These added properties may reduce interaction of the liposome with plasma proteins (including opsonin molecules) and recognition and uptake by macrophages of the reticuloendothelial system (RES).

The circulation times of liposomes are affected by the amphipathic PEG concentration [7] and PEG chain length [8]. Liposome size is also an important parameter. Only relatively small liposomes with amphipathic PEG ($d \leq 200$ nm) were long-circulating; large liposomes ($d > 200$ nm) accumulate in spleen [7]. Very small liposomes ($d \sim 50$ nm) revealed elevated accumulation in liver (Mori, A. and Huang, L., unpublished data). Therefore, there appears to be a liposome size 'window' for avoidance of RES uptake. It has been proposed that elevated liver accumulation of small liposomes may result from passage of the liposomes through the fenestrated liver endothelium, and these liposomes may then localize with the parenchymal cells [9].

The present studies further characterize the size dependence of liposome biodistribution and furthermore give insight into the mechanisms of RES uptake for amphipathic dioleoyl-*N*-(monomethoxypoly(ethylene glycol)succinyl)phosphatidylethanolamine (PEG-PE)-containing liposomes. The biodistribution of intravenously injected liposomes was monitored by following a radioactive lipid phase marker [10]. The localization of liposomes within tissues was revealed using fluorescence microscopy, where the liposomes were labeled with the lipophilic carbocyanine dye 1,1′-dioctadecyl-3,3,3′,3′-tetramethylindocarbocyanine perchlorate (DiI). DiI has low toxicity, integrates with high stability in liposome membranes [11], is resistant to transfer between cell membranes through aqueous medium [12], and does not leave macrophages after liposome uptake [11]. We report here that the liposome circulation time and biodistribution, and the steric barrier activity of PEG-PE, are liposome size dependent. Liposomes accumulated in liver, however, were localized to Kupffer cells regardless of liposome size when examined by the fluorescence microscopy technique. Even the small liposomes were localized to these macrophages, and did not appear in regions composed of parenchymal cells. The intraorgan distribution was examined for large PEG-PE-containing liposomes which accumulate in spleen. The longest-circulating liposomes experience increased tumor uptake, and the distribution of these liposomes within solid tumor was examined. These studies are relevant for the optimal design of long-circulating liposomes for drug delivery.

2. Materials and methods

2.1. Materials

EPC was purchased from Avanti Polar Lipids (Alabaster, AL), and Chol and streptavidin were obtained from Sigma (St. Louis, MO). DiI was purchased from Molecular Probes (Eugene, OR). Anti-rat IgG-FITC was obtained from Boehringer Mannheim (Indianapolis, IN). $^{111}InCl_3$ (carrier-free) was from New England Nuclear (Boston, MA). All other chemicals were of reagent grade. PEG-PE, with PEG of molecular weight 5000, was synthesized as described [1]. DTPA-SA was synthesized as described [13], and ^{111}In-labeled DTPA-SA (^{111}In-DTPA-SA) was prepared as described [14]. This lipophilic radiolabel is not transferred to serum components from liposomes [15] and is not rapidly metabolized in vivo [10]. Biotin-cap-PE was synthesized as described [16]. Monoclonal antibody F4-80, of the rat IgG_{2b} subclass, was a kind gift from Dr. G. Kraal, Department of Cell Biology, Medical Faculty, Vrije Universiteit, Amsterdam. The MC-38 C57BL/6 mouse colonic adenocarcinoma cell line was a kind gift of Dr. J. Schlom, National Cancer Institute, NIH, Bethesda, MD.

2.2. Liposome preparation

Lipid mixtures containing trace amounts of ^{111}In-DTPA-SA or hexadecyl [^{3}H]cholestanyl ether (^{3}H-CE) were dried from organic solvent with N_2 gas and vacuum desiccated for 2 h. The lipid films were allowed to hydrate in PBS, pH 7.5, at 4°C overnight. Liposomes were then prepared by extrusion through two stacked Nuclepore membranes six times. 1.0 μm pore size membranes were used to generate liposomes with average diameters > 300 nm. 0.2-μm pore size membranes were used to generate liposomes with average diameters of 150–200 nm. Small liposomes were prepared by sonicating the hydrated lipid films in a bath-type sonicator (Laboratory Supplies, Hicksville, NY) for 15 min, followed by a 15 min resting period, and an additional 15 min of sonication. After 2 h of resting to allow for annealing, homogenous sized liposomes with average diameters < 70 nm were isolated by chromatography on a Bio-Gel A-50m column equilibrated and eluted with PBS (pH 7.5). The average diameters of the liposome preparations were measured using a Coulter N4SD submicron particle size analyzer (Hialeah, FL). Liposome size was verified by negative stain electron microscopy as described [17].

2.3. Biodistribution studies

^{111}In-DTPA-SA labeled liposomes (200 μg of lipid in 200 μl PBS (pH 7.5), unless otherwise indicated)

were injected into female C57BL/6 mice (6–8 weeks old) via the tail vein. At the indicated time interval, the mice were anesthetized, weighed, and bled by retro-orbital puncture. The mice were killed by cervical dislocation and dissected. In addition to blood, organs were collected, weighed, and analyzed for ^{111}In radioactivity in a gamma counter. The results are presented as percent of the total injected dose for each organ. The total radioactivity in blood was determined by assuming that the total blood volume was 7.3% of the body weight [18]. Blood correction factors for each organ were determined as described [19] for female C57BL/6 mice of the same age and weight. Approximately 8, 9, and 1% of the total blood remained in the lung, liver, and spleen, respectively, following bleeding.

2.4. Fluorescence microscopy

Liposomes were labeled during vortexing by addition of DiI (2.5 mg/ml in 100% ethanol, 3.75 μg DiI/0.5 mg of lipid) as described [11]. The labeled liposomes were injected into mice via the tail vein (0.5 mg of lipid in 0.5 ml PBS (pH 7.5)). At 24 h post injection tissues were removed, immediately frozen in liquid nitrogen, and stored at −20°C. Tissue sections of 8 μm thickness were cut using a Reichert-Jung cryostat, placed onto poly(L-lysine) coated slides, and immediately observed and photographed using a Nikon Microphot-FX fluorescence microscope. Immunolabeling was performed as described [20] with slight modification. Briefly, slides were dried overnight over desiccant, fixed in acetone for 10 min at room temperature, and air dried. The slides were then incubated with monoclonal antibody F4-80 for 1 h at room temperature. After rinsing the slides three times with PBS (pH 7.5), they were incubated with anti-rat IgG-FITC for 1 h at room temperature. The slides were again rinsed three times with PBS (pH 7.5) and mounted using Gel/mount™ (Biomeda). DiI and FITC fluorescence were observed as yellow and green, respectively, with 'FITC optics' (excitation filter: EX450–490, dichroic mirror: DM510, and barrier filter: BA515IF). DiI fluorescence was observed as red with 'rhodamine optics' (excitation filter: EX546/10, dichroic mirror: DM580, and barrier filter: BA590).

2.5. Tumor studies

Female C57BL/6 mice were injected subcutaneously in the scapular region with $1 \cdot 10^6$ MC-38 cells. Solid tumors were evident 7–9 days post injection. At 9 days post injection, mice were injected via the tail vein with ^{111}In-DTPA-SA/DiI labeled liposomes (0.5 mg of lipid in 0.5 ml of PBS (pH 7.5)). The mice were killed at 24 h post injection, and the solid tumor analyzed for radioactivity and DiI fluorescence as described above.

2.6. Serum protein binding assay

Serum was isolated from female C57BL/6 mice by collecting blood via retro-orbital puncture, allowing the blood to coagulate at room temperature for 10 min, and centrifuging using an IEC HN-SII (Needham Hts., MA) model centrifuge (2,750 rpm, 15 min, 4°C). The supernatant was removed and further centrifuged in an Eppendorf 5415C model centrifuge (14000 rpm, 10 min, 4°C). 0.5 ml of isolated serum was immediately prewarmed by incubation in a water bath set at 37°C for 5 min. 0.5 ml of ^{3}H-CE labeled liposomes (0.5 mg of lipid in PBS (pH 7.5)) were added to the prewarmed serum and the mixture was incubated at 37°C for 30 min. The mixture was then chromatographed on a Bio-Gel A-5m column (67 cm × 0.9 cm) equilibrated and eluted with PBS, pH 7.5 at 4°C. Lipid and protein in the peak fraction eluting in the void volume were assayed by scintillation counting and the Lowry assay [21], respectively.

2.7. Streptavidin binding assay

Streptavidin was radiolabeled with ^{125}I using Iodogen (Pierce, Rockford, IL), and purified using a Bio-Gel P-4 spin column. Binding of streptavidin to biotinylated liposomes was assayed as described [7]. Briefly, 2 μg of streptavidin (1 mg/ml in PBS (pH 7.5), containing a trace of ^{125}I-streptavidin) was added to 100 μg ^{111}In-DTPA-SA labeled liposomes, which contained 2.5 mol% biotin-cap-PE in the lipid composition, in 0.5 ml PBS (pH 7.5). The mixture was incubated at room temperature for 10 min, and chromatographed on a Bio-Gel A-5m column equilibrated and eluted with PBS (pH 7.5). ^{125}I cpm eluting with the liposomes in the void volume was considered bound streptavidin, and the streptavidin to lipid weight ratio was determined from the ^{125}I cpm and ^{111}In cpm eluting as a peak in the void volume.

3. Results

3.1. Effect of liposome size on biodistribution

The primary focus of the studies described here was to investigate the intrahepatic distribution of small PEG-PE-containing liposomes by fluorescence microscopy. The distribution of these liposomes in C57BL/6 mice, used in the fluorescence studies, was therefore examined. Liposomes composed of EPC/Chol/PEG-PE (10:5:1, mol/mol) and of different sizes were prepared and injected i.v. The biodistribution results, following the lipid phase marker ^{111}In-DTPA-SA, are presented in Fig. 1. As previously reported [1,7,8], PEG-PE effectively prolonged the circulation of

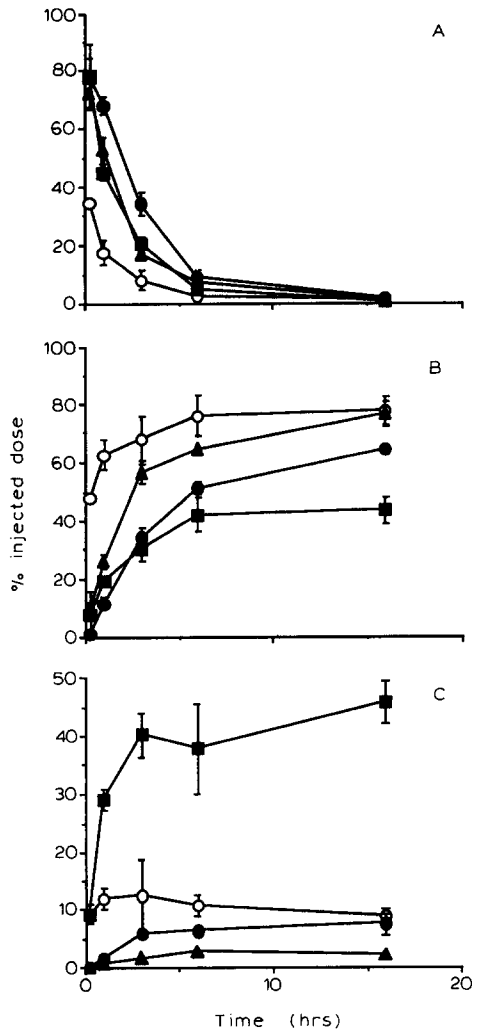

Fig. 1. Biodistribution of PEG-PE-containing liposomes of different sizes. EPC/Chol (2:1, 194 (±65) nm) liposomes (○) and EPC/Chol/PEG-PE (10:5:1) liposomes of different sizes (338 (broad) nm (■), 157 (±46) nm (●), and 67.8 (broad) nm (▲)) labeled with ^{111}In-DTPA-SA were injected i.v. (200 μg of lipid in 200 μl). Percent injected dose in blood (A), liver (B), and spleen (C) were measured at the indicated time intervals. Bars represent S.D. ($n = 3$).

EPC/Chol liposomes (Fig. 1A) by decreasing liver uptake (Fig. 1B), for liposomes with an average diameter within the range of 150–200 nm. However, when the average diameter of the PEG-PE-containing liposomes was > 300 nm, the circulation time was decreased relative to the 150–200 nm liposomes. These large liposomes accumulated efficiently in spleen (Fig. 1C) as previously reported [7]. Fig. 1C shows that this accumulation in spleen reached a saturation level of ~ 40% of the injected dose by 2.5 h post injection. Conversely, decreasing the average liposome size to < 70 nm greatly changed the resulting biodistribution. While the circulation time revealed was comparable to the large liposomes, these very small liposomes did not accumulate in spleen, and accumulated more rapidly and to higher levels in liver (Fig. 1B) compared to larger liposomes. These results confirm previous observations using other mouse strains [7].

Thus, the biodistribution of EPC/Chol/PEG-PE liposomes, as determined from the radioactive marker, was liposome size dependent. Liposomes with a diameter of 150–200 nm revealed the most prolonged circulation, while large ($d > 300$ nm) and very small ($d < 70$ nm) liposomes accumulated in spleen and liver, respectively.

3.2. Tissue distribution of liposomes

To examine the localization of liposomes within tissues, and to give insight into the mechanism of liposome uptake by various tissues, the lipophilic carbocyanine dye DiI was used as a fluorescent liposome marker. Fluorescence microscopy was thus utilized to examine the spleen and liver uptake of the large and very small EPC/Chol/PEG-PE liposomes, respectively.

Fig. 2A is a fluorescence micrograph of a section of spleen from a mouse injected with large ($d > 300$ nm) DiI labeled liposomes. The spleen was removed and frozen at 24 h post injection. In this procedure, rhodamine optics were used and the DiI fluorescence appeared red. Fluorescence was evident in the red pulp and marginal zone, and this fluorescence appeared clustered. Little or no fluorescence was observed in the white pulp.

The uptake of liposomes by liver was then investigated. To better identify cell types in the liver sections, immunolabeling was performed. The tissue sections were incubated with F4-80, a rat monoclonal antibody which binds to mouse macrophage [22]. Goat anti-rat IgG-FITC was used as secondary antibody. When examining the tissues with FITC optics, the DiI and FITC fluorescence appeared as yellow and green, respectively. It should be noted here that the degree of background fluorescence from liver under FITC optics varies significantly with mouse strain. BALB/c liver sections revealed a high degree of green autofluorescence masking the FITC labeled antibody. Liver sections from C57BL/6 mice gave negligible background fluorescence. This mouse strain was therefore used for these and all studies described above.

Fig. 2B is a fluorescence micrograph of an immunolabeled liver section from a mouse injected with DiI labeled EPC/Chol liposomes with an average diameter of 180 (±38) nm. The liver was removed at 24 h post injection. The Kupffer cells are clearly marked with green fluorescence. In this section, as well as in immunolabeled liver sections from mice injected with DiI labeled EPC/Chol/PEG-PE liposomes of different sizes (Figs. 2C–E), yellow fluorescence was found only with green fluorescence. To confirm the localization of liposomes within the tissue section, the epi-fluo-

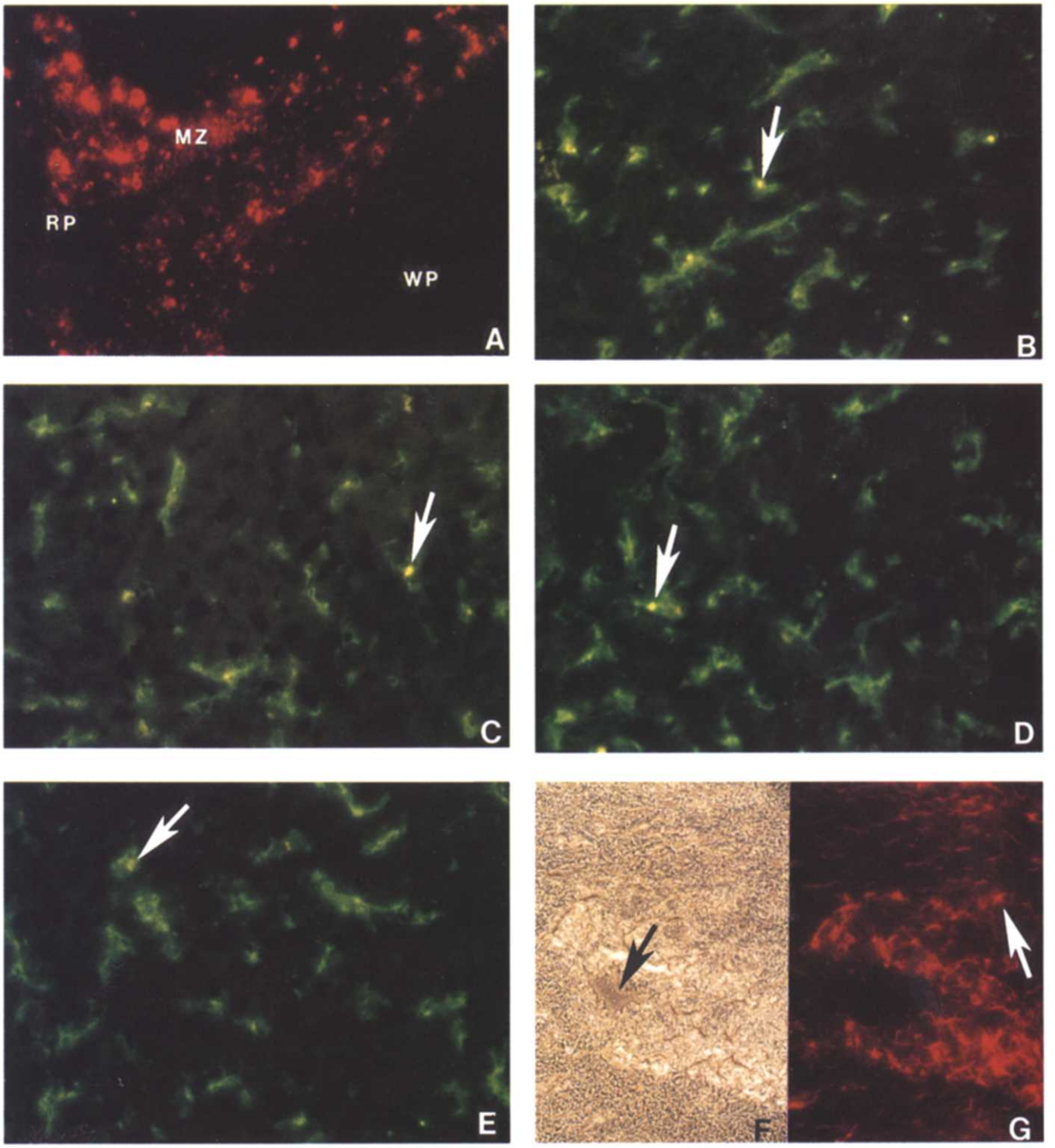

Fig. 2. Localization of liposomes in tissues. Mice were injected with DiI-labeled liposomes (3.75 μg DiI/0.5 mg of lipid in 0.5 ml) and killed at 24 h post injection. (A) Fluorescence micrograph of spleen cryosection from a mouse injected with EPC/Chol/PEG-PE liposomes (10:5:1, 366 (broad) nm), viewed with rhodamine optics. Magnification: ×195. RP, red pulp; WP, white pulp; and MZ, marginal zone. (B–E) Fluorescence micrographs of liver cryosections from mice injected with EPC/Chol (2:1, 180 (±38) nm) liposomes (B), or EPC/Chol/PEG-PE (10:5:1) liposomes of different sizes (C, 366 (broad) nm; D, 167 (±52) nm, and E, 63.9 (broad) nm). Kupffer cells were immunolabeled with F4-80 and FITC-labeled secondary antibody. Sections were viewed with FITC optics, ×195. Arrows indicate FITC-labeled Kupffer cells with additional (DiI) yellow fluorescence. (F) Phase contrast micrograph, and (G) corresponding fluorescence micrograph of MC-38 tumor cryosection from mice injected with EPC/Chol/PEG-PE liposomes (10:5:1, 151 (±45) nm). (G) viewed with rhodamine optics. Magnification of (F) and (G): ×195. Arrows indicate blood vessel (F) and liposome extravasation (G).

Table 1
Effect of PEG-PE and liposome size on serum protein binding and tumor accumulation of liposomes

Lipid composition	Diameter (S.D.) in nm	Protein/lipid (wt/wt) [a]	% Injected dose per g tumor [b]
EPC/Chol/PEG-PE	412 (broad)	$< 1.97 \cdot 10^{-3}$	–
EPC/Chol/PEG-PE	151 (39)	$5.28 \cdot 10^{-3}$	5.1 (0.8)
EPC/Chol/PEG-PE	59.5 (broad)	$2.35 \cdot 10^{-1}$	–
EPC/Chol	169 (54)	$4.49 \cdot 10^{-1}$	2.8 (0.3) [c]

[a] Liposomes composed of EPC/Chol/PEG-PE (10 : 5 : 1) or EPC/Chol (2 : 1) and labeled with ^{3}H-CE were incubated with 50% mouse serum for 30 min at 37°C. The samples were then applied to a Bio-Gel A5m column at 4°C. Lipid and protein in the peak fraction eluting in the void volume were assayed by scintillation counting and the Lowry assay, respectively.
[b] Mice (female C57BL/6 injected with $1 \cdot 10^{6}$ MC-38 tumor cells 9 days prior) were injected with ^{111}In-DTPA-SA labeled liposomes (0.5 mg of lipid in 0.5 ml). Mice were killed 24 h post injection. Values represent % injected dose per g of tumor. Numbers in parentheses indicate S.D. ($n = 3$).
[c] Significantly different from EPC/Chol/PEG-PE liposomes ($p < 0.025$).

rescence filter apparatus was switched to rhodamine optics, where only fluorescence from DiI was detectable (micrographs not shown). Even for the very small EPC/Chol/PEG-PE liposomes (Fig. 2E), DiI fluorescence was observed with Kupffer cells, and no fluorescence was visible in areas without Kupffer cells. Similar results were observed for mice killed at earlier time points (micrographs not shown). Although some DiI fluorescence was lost during fixation, adequate fluorescence remained in the tissue and was specifically localized to the Kupffer cells.

Therefore, these studies indicate that PEG-PE liposomes, regardless of size, localize with Kupffer cells when taken up from the circulation by liver. Even the longest circulating PEG-PE-containing liposomes ($d \sim$ 150–200 nm) eventually localize with Kupffer cells when taken up by liver (Fig. 1B). This data further suggests that the very small ($d < 70$ nm) liposomes do not reach the parenchymal cells.

3.3. Serum protein binding

Differences in clearance rates of the liposomes from the circulation may be related to differences in their susceptibility for opsonization. To explore this possibility, the binding of serum proteins to the liposomes was examined. The results are presented in Table 1 as protein to lipid weight ratios of isolated serum-incubated liposomes. PEG-PE reduced the amount of bound protein nearly 100-fold for EPC/Chol liposomes with an average diameter of 150–200 nm. Furthermore, the extent of serum protein binding to EPC/Chol/PEG-PE liposomes varied with liposome size. The amount of bound protein was below the detection limit of the assay for large liposomes. Possible multilamellarity in the large liposome preparation, however, may have led to an underestimate of the bound protein. Conversely, the very small liposomes ($d \sim 60$ nm) bound protein much more avidly than the larger PEG-PE-containing liposomes, where the ratio of protein to lipid increased to approximately 45-fold more than for the liposomes with an average diameter of 151 ($\pm$39) nm. Thus, while PEG-PE reduces serum protein binding, this reduction is liposome size dependent.

3.4. Streptavidin binding

PEG-PE may reduce opsonization of liposomes by providing a steric barrier. To investigate the steric barrier provided by PEG-PE with regard to liposome size, EPC/Chol/PEG-PE liposomes of different sizes and containing biotin-cap-PE in the lipid composition were prepared, and the ability of the liposomes to bind streptavidin examined. For liposomes containing 2.5 mol% PEG-PE, streptavidin was avidly bound and there was no liposome size dependence (Table 2). However, a liposome size dependence was observed when the concentration of PEG-PE was increased to 5.0 mol%. Though the amount of streptavidin bound to the very small liposomes was greatly decreased, these liposomes bound approximately 20% of the available streptavidin, with a final streptavidin to lipid weight ratio of $6.2 \cdot 10^{-3}$. This binding was completely blocked by addition of excess free biotin. Larger liposomes

Table 2
Effect of PEG-PE and liposome size on binding of streptavidin to liposomes additionally containing biotin-cap PE [a]

Mol% PEG-PE	Diameter (S.D.) in nm	% Streptavidin bound [b]	ng Streptavidin per μg lipid [c]
0	302 (broad)	69.6	16.8
0	145 (51)	67.9	16.6
0	67.7 (broad)	61.1	16.6
2.5	563 (broad)	58.1	14.6
2.5	152 (51)	62.8	15.7
2.5	63.8 (broad)	55.5	15.9
5.0	408 (broad)	2.7	0.7
5.0	151 (38)	2.7	0.7
5.0	68.5 (broad)	21.6	6.2
7.5	305 (broad)	3.9	0.9
7.5	161 (55)	5.5	1.3
7.5	61.8 (broad)	17.9	5.7

[a] Liposomes composed of EPC/Chol (2 : 1) and additionally containing 2.5 mol% biotin-cap-PE and the indicated mol% of PEG-PE were incubated with ^{125}I-streptavidin at room temperature for 10 min. The mixtures were then chromatographed on a Bio-Gel A5m column to remove unbound streptavidin.
[b] ^{125}I cpm eluting with the ^{111}In-DTPA-SA labeled liposomes was considered bound streptavidin.
[c] Weight ratio based on ^{125}I cpm and ^{111}In cpm in the eluting liposome peak.

bound approx. 3% of the available streptavidin. A similar size dependence for streptavidin binding was observed when the concentration of PEG-PE was further increased to 7.5 mol%, with a slight decrease in streptavidin binding by the very small liposomes. No liposome size dependence was observed for streptavidin binding to liposomes without PEG-PE. Thus, these results indicate that with a sufficient concentration of PEG-PE, a difference in the ability of the polymer to reduce protein binding exists with regard to liposome size.

3.5. Liposome accumulation in solid tumor

Solid tumors were grown in C57BL/6 mice by s.c. injection of MC-38 cells in the scapular region. These cells were of the MC-38 C57BL/6 mouse adenocarcinoma cell line [23]. Liposomes labeled with ^{111}In-DTPA-SA were injected i.v. into tumor bearing mice, and at 24 h post injection the tumors were excised and the radioactivity measured. The presence of PEG-PE in EPC/Chol liposomes, with an average diameter of 150–200 nm, nearly doubled the % injected dose accumulated/g tumor (Table 1). Thus, the EPC/Chol/PEG-PE (10:5:1, mol/mol) liposomes, of a size which revealed the most prolonged circulation, accumulated more efficiently in the MC-38 solid tumor than the conventional liposomes.

3.6. Liposome distribution within solid tumor

To examine the localization of the liposomes within the MC-38 tumors, DiI-labeled EPC/Chol/PEG-PE liposomes (151 ($\pm$45) nm) were injected into tumor bearing mice, and the tumors excised at 24 h post injection. This size range of liposomes was chosen because they exhibited an elevated level of tumor accumulation (Table 1). Microscopic analysis of tumor sections revealed several blood vessels of various diameters within the tumor mass. A phase contrast micrograph (Fig. 2F) and the corresponding fluorescence micrograph (Fig. 2G) reveal the liposome distribution within the tumor. The fluorescence is most intense surrounding blood vessels. The fluorescence intensity greatly decreased into the tumor mass and away from the blood vessels. However, fluorescence is detectable beyond the endothelial layer (arrow, Fig. 2G), indicating some extravasation of liposomes.

4. Discussion

Prolongation of liposome circulation by the addition of PEG-PE to the liposome composition may greatly advance the therapeutic potential of liposomes as drug carriers. However, the long-circulating behavior of these liposomes is restricted within certain parameters. PEG-PE prolongs liposome circulation for a variety of lipid compositions [24], yet when DOPE is the major matrix lipid the circulation time is reduced and high spleen accumulation occurs [17]. Another parameter which can restrict the circulation of PEG-PE-containing liposomes (PEG-PE liposomes) is liposome size. To investigate the role of liposome particle size in determining PEG-PE liposome biodistribution, liposomes of three characteristic sizes were compared. These sizes included liposomes with average diameters of >300 nm, 150–200 nm, and <70 nm.

Large liposomes with an average diameter >200 nm and containing PEG-PE have previously been shown to accumulate in spleen [7]. The red pulp of the spleen consists of a meshwork of reticular fibers with reticular cells accompanied by fixed macrophages. Aged or damaged red blood cells are thereby filtered in this meshwork and are ingested by the splenic macrophage. The present studies show that the accumulation of large PEG-PE liposomes ($d > 300$ nm) is rapid and reaches steady state by 2.5 h post injection. Furthermore, fluorescence microscopy revealed that these liposomes localize in the red pulp and marginal zone. Together these results indicate liposome uptake via a filtration mechanism. It has been proposed that large G_{M1}-containing liposomes ($d > 300$ nm) accumulate in spleen by filtration and are taken up by spleen macrophages [25]. Preliminary immunolabeling studies revealed spleen macrophage uptake of the large PEG-PE liposomes (Litzinger, D., et al., unpublished data).

Vessels in solid tumors are in general considered to be inherently leaky, reportedly having exceptionally fenestrated endothelium [26]. Despite having relatively low aqueous volume for encapsulation [27], small PEG-PE liposomes would be expected to better extravasate beyond the endothelial layer in tumor vessels, thereby serving as more efficient drug carriers. However, small PEG-PE liposomes ($d < 70$ nm) were more rapidly cleared from the circulation than the long-circulating PEG-PE liposomes ($d \sim 150$–200 nm). This more rapid clearance by liver would expectedly reduce the opportunity for the small liposomes to accumulate in tumor. Tumor accumulation of small G_{M1}-containing liposomes ($d < 70$ nm) was greatly reduced from that of relatively longer circulating G_{M1}-liposomes ($d \sim 70$–200 nm) [9]. Other investigators have shown that smaller liposomes are retained in circulation to higher levels after injection than larger liposomes [5,24]. However, one study compared liposomes within the size range of 100–250 nm [24]. Another compared the ratio of large (182 ($\pm$58) nm) to small (80 ($\pm$12) nm) liposomes injected and then reisolated in plasma [5]. The liposome sizes compared in the present study are beyond this range, and their behavior may differ from the trends shown within the more narrow range. Further-

more, a slight discrepancy (within 10 nm) was found when measuring particle size by electron microscopy. These measurements indicate that the very small liposomes are even smaller than what is measured by quasi-elastic light scattering. The other studies further differed in that lower molar percentages of PEG-PE, with PEG of molecular weight 1900 derivatized with DSPE, were included in the lipid compositions [5,24].

The main issue of the present studies was to investigate the loss of long-circulation behavior with the small PEG-PE liposomes. Because the endothelial lining of the liver sinusoids includes fenestrae with an average diameter of 100 nm [28], the small PEG-PE liposomes might be expected to penetrate through these fenestrations and gain access to the hepatocytes. This would be in agreement with previous reports that small unilamellar liposomes (without PEG-PE) could accumulate in parenchymal cells of the liver [29,30]. However, the results using fluorescence microscopy revealed localization of the small PEG-PE liposomes ($d < 70$ nm) only to Kupffer cells. Parenchymal cells, however, constitute 92.5% of the total hepatocellular volume [31]. Detection of liposome uptake by hepatocytes using this technique may therefore be limited, as these cells are spread over a relatively large area, and any associated fluorescence may be dispersed and below the sensitivity for detection. Other techniques, such as cell isolation and fractionation [30], may help to reveal the cell type in the liver which takes up the small PEG-PE liposomes.

Similar localization results were obtained for the long-circulating PEG-PE liposomes ($d \sim 150$–200 nm), where fluorescence was observed only with the Kupffer cells. These liposomes would not be expected to reach the parenchymal cells due to their larger size. It can therefore be suggested that PEG-PE may act by merely slowing the eventual uptake of EPC/Chol liposomes by the Kupffer cells.

The present studies show that the more rapid uptake of small PEG-PE liposomes may actually result from less resistance to opsonization relative to long-circulating PEG-PE liposomes. Inclusion of G_{M1} in sphingomyelin/EPC liposomes has been shown to prolong liposome circulation, with a corresponding decrease in the amount of protein associated with reisolated liposomes [32]. PEG-coating of liposomes has been shown to reduce adsorption of plasma components in vitro [33]. The present studies have shown that small PEG-PE liposomes adsorb protein from mouse serum to a greater extent than the long-circulating PEG-PE liposomes (Table 1). These results may suggest more avid adsorption of protein, possibly including opsonin(s), to small PEG-PE liposomes in vivo, leading in turn to a more rapid clearance from the circulation. Results from the streptavidin binding assay further and more directly reveal that the ability of PEG-PE to reduce protein binding is significantly decreased for the small liposomes (Table 2). A possible explanation for these results is that as the curvature of the liposome is increased, the extended chains splay to a greater degree, analogous to an increase in the spacing between bristles of a hair brush. Thus, protein (including opsonin(s)) can more easily penetrate the more highly splayed polymer chains of the small liposomes.

PEG-PE was shown here to enhance liposome accumulation in solid tumor, in agreement with previous reports using a similar tumor model [4,6]. This likely resulted from prolonged circulation and extravasation through the leaky endothelial barrier of the tumor vessels. Fluorescence microscopy revealed some extravasation of the liposomes into the tumor mass. These liposomes may therefore be expected to carry drug into the tumor mass. The MC-38 cell line used in these studies has recently been transduced with cDNA encoding the human carcinoembryonic antigen (CEA) gene [34]. The ability of the CEA transduced cell line MC-38-cea2 to grow as tumors in mice, and the ability of anti-CEA monoclonal antibody to target these tumors [35], should provide further approaches for this model system to study tumor targeting of and therapy by long-circulating liposomes.

5. Acknowledgments

This work was supported by NIH grant CA24553. A.M.J.B. is supported by NWO grant: 900-505-224. Travel of A.M.J.B. was supported by Mallinckrodt Medical, Inc. (St. Louis, MO). D.C.L. was a Ph.D. student in the Department of Biochemistry at the University of Tennessee, Knoxville, TN.

6. References

[1] Klibanov, A.L., Maruyama, K., Torchilin, V.P. and Huang, L. (1990) FEBS Lett. 268, 235–237.
[2] Blume, G. and Cevc, G. (1990) Biochim. Biophys. Acta 1029, 91–97.
[3] Allen, T.M., Hansen, C., Martin, F., Redemann, C. and Yau-Young, A. (1991) Biochim. Biophys. Acta 1066, 29–36.
[4] Papahadjopoulos, D., Allen, T.M., Gabizon, A., Mayhew, E., Matthay, K., Huang, S.K., Lee, K.D., Woodle, M.C., Lasic, D.D., Redemann, C. and Martin, F.J. (1991) Proc. Natl. Acad. Sci. USA 88, 11460–11464.
[5] Huang, S.K., Lee, K.D., Hong, K., Friend, D.S. and Papahadjopoulos, D. (1992) Cancer Res. 52, 5135–5143.
[6] Huang, S.K., Mayhew, E., Gilani, S., Lasic, D.D., Martin, F.J. and Papahadjopoulos, D. (1992) Cancer Res. 52, 6774–6781.
[7] Klibanov, A.L., Maruyama, K., Beckerleg, A.M., Torchilin, V.P. and Huang, L. (1991) Biochim. Biophys. Acta 1062, 142–148.
[8] Mori, A., Klibanov, A.L., Torchilin, V.P. and Huang, L. (1991) FEBS Lett. 284, 263–266.
[9] Liu, D., Mori, A. and Huang, L. (1992) Biochim. Biophys. Acta 1104, 95–101.

[10] Holmberg, E., Maruyama, K., Litzinger, D.C., Wright, S., Davis, M., Kabalka, G.W., Kennel, S.J. and Huang, L. (1989) Biochem. Biophys. Res. Commun. 165, 1272–1278.
[11] Claassen, E. (1992) J. Immunol. Methods 147, 231–240.
[12] Honig, M.G. and Hume, R.I. (1989) Trends Neurosci. 12, 333–341.
[13] Kabalka, G.W., Buonocore, E., Hubner, K., Moss, T., Norley, N. and Huang, L. (1987) Radiology 163, 255–258.
[14] Maruyama, K., Kennel, S.J. and Huang, L. (1990) Proc. Natl. Acad. Sci. USA 87, 5744–5748.
[15] Kabalka, G.W., Davis, M.A., Moss, T.H., Buonocore, E., Hubner, K., Holmberg, E., Maruyama, K. and Huang, L. (1991) Magn. Reson. Med. 19, 406–415.
[16] Bayer, E.A., Rivnay, B. and Skutelsky, E. (1979) Biochim. Biophys. Acta 550, 464–473.
[17] Litzinger, D.C. and Huang, L. (1992) Biochim. Biophys. Acta 1127, 249–254.
[18] Wu, M.S., Robbins, J.C., Bugianesi, R.L., Ponpipom, M.M. and Shen, T.Y. (1981) Biochim. Biophys. Acta 674, 255–258.
[19] Litzinger, D.C. and Huang, L. (1992) Biochim. Biophys. Acta 1104, 179–187.
[20] Buiting, A.M.J., De Rover, Z., Claassen, E. and Van Rooijen, N. (1993) Immunobiology 188, 13–22.
[21] Lowry, O.H., Rosebrough, N.J., Farr, A.L. and Randall, R.J. (1951) J. Biol. Chem. 193, 265–275.
[22] Austyn, J.M. and Gordon, S. (1981) Eur. J. Immunol. 11, 805–815.
[23] Fox, B.A., Spiess, P.F., Kasid, A., Puri, R., Mule, J.J., Weber, J.S. and Rosenberg, S.A. (1990) J. Biol. Response Modif. 9, 499–511.
[24] Woodle, M.C., Matthay, K.K., Newman, M.S., Hidayat, J.E., Colins, L.R., Redemann, C., Martin, F.J. and Papahadjopoulos, D. (1992) Biochim. Biophys. Acta 1105, 193–200.
[25] Liu, D., Mori, A. and Huang, L. (1991) Biochim. Biophys. Acta 1066, 159–165.
[26] Granger, D.N. and Perry, M.A. (1983) Physiol. Pharmacol. Microcirc. 1, 157–208.
[27] Lichtenberg, D., Friere, E., Schmidt, C.F., Barenholz, Y., Felgner, P.L. and Thompson, T.E. (1981) Biochemistry 20, 3462–3467.
[28] Wisse, E. (1970) J. Ultrastruct. Res. 31, 125–150.
[29] Hwang, K.J., Luk, K.F.S. and Beaumier, P.L. (1980) Proc. Natl. Acad. Sci. USA 77, 4030–4034.
[30] Roerdink, F., Regts, J., Van Leeuwen, B. and Scherphof, G. (1984) Biochim. Biophys. Acta 770, 195–202.
[31] Blouin, A., Bolender, R.P. and Weibel, E.R. (1977) J. Cell Biol. 72, 441–455.
[32] Chonn, A., Semple, S.C. and Cullis, P.R. (1992) J. Biol. Chem. 267, 18759–18765.
[33] Senior, J., Delgado, C., Fisher, D., Tilcock, C. and Gregoriadis, G. (1991) Biochim. Biophys. Acta 1062, 77–82.
[34] Robbins, P.F., Kantor, J.A., Salgaller, M., Hand, P.H., Fernsten, P.D. and Schlom, J. (1991) Cancer Res. 51, 3657–3662.
[35] Hand, P.H., Robbins, P.F., Salgaller, M.L., Poole, D.J. and Schlom, J. (1993) Cancer Immunol. Immunother. 36, 65–75.